Experimental Thermal and Fluid Science 52 (2014) 288–296

Contents lists available at ScienceDirect

Experimental Thermal and Fluid Science

journal homepage: www.elsevier.com/locate/etfs

Measurement on instantaneous flame front structure of turbulent premixed CH_4/H_2/air flames

Meng Zhang [a], Jinhua Wang [a,*], Yongliang Xie [a], Zhilong Wei [a], Wu Jin [a], Zuohua Huang [a,*], Hideaki Kobayashi [b]

[a] State Key Laboratory of Multiphase Flow in Power Engineering, Xi'an Jiaotong University, Xi'an 710049, PR China
[b] Institute of Fluid Science, Tohoku University, Sendai, Miyagi 980-8577, Japan

ARTICLE INFO

Article history:
Received 16 June 2013
Received in revised form 4 October 2013
Accepted 6 October 2013
Available online 15 October 2013

Keywords:
Hydrogen addition
Turbulent burning velocity
Flame front structure
Flame surface density
OH-PLIF

ABSTRACT

Instantaneous flame front structure of turbulent premixed CH_4/H_2/air flames (hydrogen fraction of 0%, 5%, 10% and 20% by mole fraction) was investigated quantitatively using a nozzle-type Bunsen burner. Hot wire anemometer and OH-PLIF were used to measure the turbulent flow and detect the instantaneous flame front structure, respectively. Turbulent burning velocity, S_T, flame surface density, Σ, and mean flame volume, V_f, were calculated by processing the OH-PLIF images. Results show that the flame front structures of the turbulent premixed flames are the wrinkled flame front and it becomes much finer with the increase of turbulence intensity as well as hydrogen fraction. The value of S_T/S_L significantly increases with the increase of u'/S_L and it slightly increases with the increase of hydrogen fraction. Flame surface density profile are symmetric and gives its maximum value at about $\langle c \rangle = 0.5$. Hydrogen addition slightly enhances the Σ and the tendency is more obvious under higher turbulence intensity. The decrease of Σ with the increase of turbulence intensity is mainly due to the effect of flame volume. The mean flame volume of flame region obviously increases with the increase of turbulence intensity within the experimental range due to the increase in depth of the large scale flame wrinkles and flame height. Hydrogen addition is not a predominant factor within the hydrogen fraction range in this study.

1. Introduction

With increasing of energy demand and concern of environmental protection, the researches on clean alternative power system have attracted a significant interest from the combustion community in recent years. Natural gas is regarded as one of the most promising clean alternative fuels and has been widely used. As the main composition of natural gas, methane has unique tetrahedral molecular structure with high C–H bond energy, thus it demonstrates some disadvantages such as slow burning velocity, poor lean-burn ability and high combustion instability [1,2]. Thus, one effective method to improve the combustion of natural gas is to mix with hydrogen which is an excellent additive to improve the combustion of hydrocarbon fuel due to its low ignition energy, high reactivity, high diffusivity and subsequently high burning velocity [3].

Previous studies of authors' group [4–6] and other groups [7] showed that a small fraction of hydrogen addition can not only significantly improve the thermal efficiency and decrease the emissions but also achieve the stable lean combustion along with low cyclic variations in engine. Experimental studies on laminar premixed flames showed that the effect of hydrogen addition on the laminar burning velocity of CH_4/H_2/air mixtures is non-linear [8]. There were also many studies on turbulent combustion of CH_4/H_2/air conducted experimentally and numerically. Fairweather et al. [9] and Nakahara et al. [10] investigated the turbulent burning velocities and the stretch effect of CH_4/H_2/air flame. Results showed that there was clear increase in turbulence burning velocity with 20% H_2 for lean mixtures. However, all experiments were conducted in a combustion chamber and the flame propagation process in the combustion chamber is essentially transient. The visualization technique such as Schlieren technique used in combustion chamber experiment is projective image information which is much different from that of the cross section planar information obtained with OH-PLIF. Meanwhile, the burner stabilized Bunsen flame can provide continuous long duration measurement which is suitable for laser diagnostic and the subsequent flame front structure analysis. Studies have also been done on the effect of hydrogen enrichment on lean flame stability [11], lean extinction [12], stability characteristics and flame structure [13] of swirling flames of CH_4/air mixtures. Moreover, a number of computational studies of lean premixed CH_4/H_2/air combustion

* Corresponding authors. Tel.: +86 29 82665075 (J. Wang); fax: +86 29 82668789.
E-mail addresses: jinhuawang@mail.xjtu.edu.cn (J. Wang), zhhuang@mail.xjtu.edu.cn (Z. Huang).

0894-1777/$ - see front matter © 2013 Elsevier Inc. All rights reserved.
http://dx.doi.org/10.1016/j.expthermflusci.2013.10.002

Nomenclature

A	area of the burner outlet, mm^2
$\langle c \rangle$	mean progress variable
$\bar{A}_f$	time-averaged surface area, mm^2
I_0	mean stretch factor
L_M	Markstein length, mm
$\bar{L}_f$	time-averaged surface length, mm
Le_{eff}	effective Lewis number
l_k	Kolmogorov microscale, mm
l_λ	Taylor microscale, mm
l_0	Integral scale, mm
l_i	flame intrinsic instability scale, mm
M_a	Markstein number
Re_λ	turbulence Reynolds number based on Taylor microscale, mm
S_L	laminar burning velocity, cm/s
S_{Lk}	local burning velocity for the stretched flame, cm/s
S_T	turbulent burning velocity, cm/s
T_{ad}	adiabatic flame temperature, K
T_b, T_u	burned and unburned mixture temperature, K
U	mean velocity of the mixtures at the burner outlet, m/s
u'	turbulence intensity, m/s
V_f	mean flame volume, mm^3
$\langle W \rangle$	averaged heat release rate
Xi	mole fraction of specific species i
Δx	interrogation box size, mm
Y_f	mass fraction of the fuel
ZH_2	hydrogen ratio, %
α_D	thermal diffusivity coefficient
ϕ	equivalence ratio
θ	angle of the contour $\langle c \rangle = 0.1$
ρ_b, ρ_u	burned and unburned mixture density, kg/m^3
Σ	flame surface density, mm^{-1}
$\dot{\omega}$	mean reaction rate
δ_L	flame thickness, mm

system focused on the flame response to local burning speeds [14], flame extinction and strained flows [12,15]. However, the effect of hydrogen addition on the flame–turbulence interaction of hydrocarbons turbulent premixed flames was still not well investigated and far from understood. The mechanism of hydrogen enrichment on improving the combustion is still not well understood and needs further study.

Moreover, turbulent combustion involves multiple processes of vastly different scales. This is manifested by complex flame front structures such as wrinkled flames, flamelets, and flame brushes [16]. Turbulent flame front structure possesses wrinkles of negative curvature surrounding large pockets of modest positive curvature, which is mainly due to the key pathways of governing reactions under the turbulent condition and they significantly differ to those under the laminar condition. These wrinkles are mainly caused by small scale turbulence interaction combined with flame instability. Flame front structure reveals the interaction between turbulence and flame, and it can also be used for turbulent combustion modeling [17]. This aspect of turbulence–chemistry interaction has not received significant attention even though it is a crucial issue in correctly describing the combustion chemistry in turbulent flows. To date, many characteristic descriptions of flame front structure have been provided, such as flame surface density [18], mean flame volume [19], geometric description (local curvature and local flamelet angle) [17] and cutoff scales in fractal theory [20]. In general, the turbulence–chemistry interaction needs far more attention than it is receiving currently. Flame front structure and turbulent burning velocity of the CH_4/H_2/air mixtures were reported by the authors [21], however the detailed flame front structure was not well investigated quantitatively and flame properties and flow structures were not yet understood.

The objective of this study is to investigate the detailed flame front structure of the turbulent premixed CH_4/H_2/air flames, with hydrogen fraction up to 20%. Both turbulence measurements by hot-wire anemometer and OH-PLIF for the turbulent premixed flames were performed to describe the flow field and instantaneous flame front structure. By analyzing the OH-PLIF images, quantitative parameters, i.e. turbulent burning velocity, S_T, flame surface density, Σ, and mean volume of turbulent flame region, V_f, were calculated. The laminar flame parameters, such as S_L, Le_{eff}, were calculated and the effects of hydrogen enrichment on flame–turbulence interaction were analyzed based on those quantitative parameters.

2. Experimental setup and procedures

Fig. 1 shows a schematic of the experimental apparatus. Experiments were conducted using a nozzle-type turbulent premixed Bunsen burner with an outlet diameter of 20 mm by using OH-PLIF technique [22]. The burner is sketched in Fig. 2. A perforated plate is installed 40 mm upstream of the nozzle outlet to generate the turbulence [23]. Turbulence parameters at nozzle outlet were measured using a constant-temperature hot-wire anemometer (Dantec, Streamline 90 N) and calculated by assuming Taylor hypothesis and isotropic turbulence assumption. Variations of Integral scale, l_0, Taylor microscale, l_λ, Kolmogorov scale, l_K, and Reynold number based on Taylor microscale, Re_λ, with turbulence intensity, u', are shown in Fig. 3. Details about the experimental setup were described in literature [21].

The mixtures were premixed in a mixing bomb and supplied into the bottom of the burner. Hydrogen fraction, ZH_2, is defined as $ZH_2 = XH_2/(XCH_4 + XH_2)$, where XH_2 and XCH_4 are the mole fractions of H_2 and CH_4, respectively. Hydrogen fractions of 0%, 5%, 10% and 20% were tested in the experiment. The laminar burning velocity, S_L, for the mixtures in this study was estimated by using the PREMIX code [24] and CHEMKIN-II database [25] with GRI-Mech 3.0 [26]. The properties of the mixtures were summarized in Table 1. δ_L is the laminar flame thickness calculated by $\delta_L = \alpha_D/S_L$, where α_D is the thermal diffusivity of the mixtures. L_M is the Markstein length calculated by $L_M = \delta_L Ma$, where Ma is the Markstein number. Effective Lewis number, Le_{eff}, and flame instability scale, l_i are calculated by the methods of Bechtold and Matalon [27] and Yuan et al. [28]. Fig. 4 shows the turbulent premixed flames of the present work in the Borghi's diagram modified by Peters [29].

OH-PLIF was used to detect the instantaneous flame front structure as shown in Fig. 1. The OH-PLIF measurement system consists of a laser source, which includes a Nd:YAG as pumping laser and a tunable dye laser, ICCD camera (LaVision Image ProX) and the software for signal control and data acquisition. The wavelength of Nd:YAG laser (Quanta-Ray Pro-190) is 355 nm with frequency of 10 Hz and energy of 300 mJ per pulse and pulse time of 10 ns. A pumped dye laser (SirahPRSC-G-3000) with a frequency doubler transfers the wavelength to 282.769 nm which is used to excite the Q1(8) line of the $A2\Sigma \leftarrow X2\Pi(1,0)$ transition with pulse energy of about 8 mJ. The laser goes through the energy monitor and sheet optics produce a laser sheet, which is about 80 mm in height and

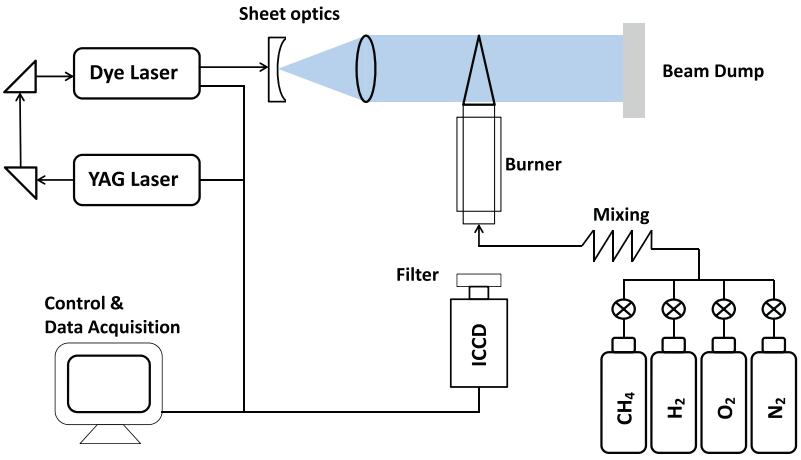

Fig. 1. Schematic of the experimental setup and PLIF system.

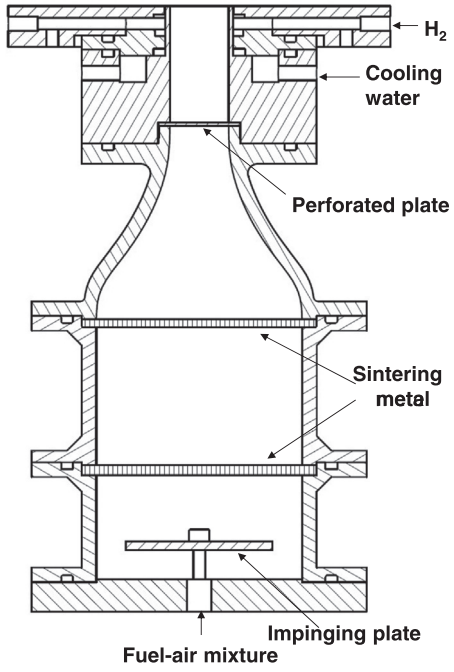

Fig. 2. Schematic of the turbulent premixed Bunsen burner.

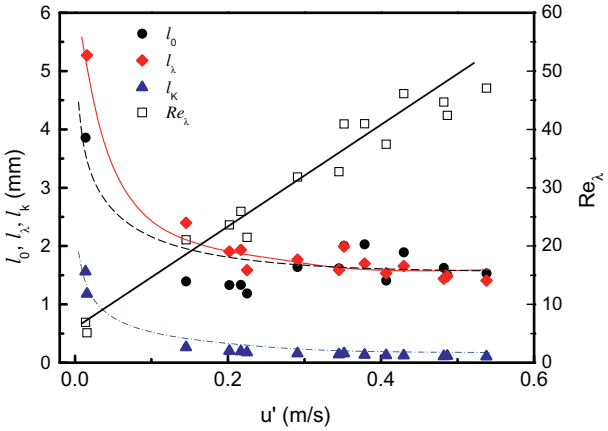

Fig. 3. Relationship between turbulence intensity, u', and scales of the turbulence; Integral scale, l_0, Taylor scale, l_λ, Komogorov scale l_K, and Reynold number based on Taylor scale, Re_λ.

Table 1
The mixture properties in this study.

ZH_2 (%)	ϕ	S_L (cm/s)	T_{ad} (K)	δ_L (mm)	L_M (mm)	ρ_b ρ_u	Le_{eff}	l_i (mm)
0	0.90	34.03	2133	0.066	0.25	0.141	0.96	1.36
5	0.88	33.91	2111	0.067	0.24	0.141	0.86	1.14
10	0.87	34.29	2100	0.067	0.24	0.144	0.79	0.98
20	0.83	33.62	2051	0.071	0.23	0.148	0.68	0.74

thickness is less than 0.5 mm, at the flame position. The ICCD camera was located perpendicularly with the laser sheet. Almost all OH-PLIF emission form the (0, 0) bands was received by the ICCD camera with the resolution of 1600 × 1200 pixel through a UV lens (Nikon Rayfact PF 10545MF-UV) with intensified Relay Optics (Lavision VC08-0094) and OH bandpass filter (LaVision VZ08-0222). The CCD camera and Relay Optics were operated with f = 4.5, 2000 μs exposure time and 200 ns gate width, 100 ns delay, 65% in gain and 10 Hz image sampling frequency synchronized with laser. The finest pixel resolution is 68 μm on the laser sheet measurement plane and the corresponding image size is very large i.e. larger than 4 Mb. Thus, binning of four pixels was performed and the resolution (about 136 μm) was verified sufficiently in this study.

3. Image processing method

Fig. 5 shows the typical single shot OH-PLIF images of the turbulent premixed flames. Image processing for the measurements of turbulent burning velocity, S_T, flame surface density, Σ, and mean flame volume, V_f, was performed for the OH-PLIF images. As shown in Fig. 6, the original RGB image is first translated from 3 × 8 bits resolution to 8 bits resolution with 256 gray intensity levels (Fig. 6a). The progress variable c is defined using the local temperature

$$c(x,y) = [T(x,y) - T_u]/(T_b - T_u) \quad (1)$$

where $T(x, y)$ is the local temperature, T_u and T_b are the unburned and burned mixture temperature, respectively. *As the temperature increases very rapidly from T_u to T_b in the flame front as the OH radical and the flame is a very thin layer in the present flamelet regime, temperature profile measurement of T_u and T_b can be indicated as OH radical detection* [30]. *Thus,* each gray image was processed by assigning one (white) to the burned region and zero (black) to the unburned

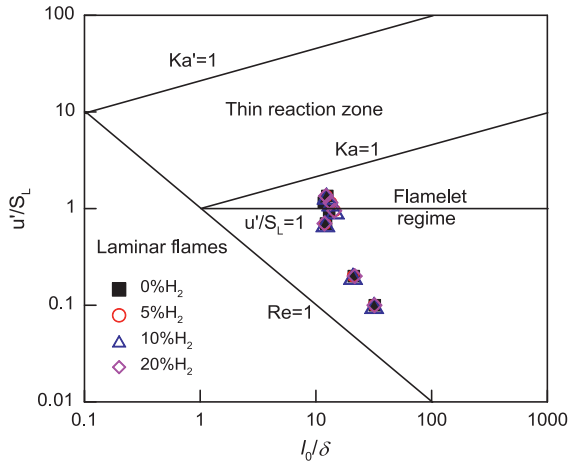

Fig. 4. Borghi's diagram of turbulent premixed flames revised by Peters [29].

region, resulting in an instantaneous binary map of the reaction progress variable, c, as shown in Fig. 6b. The flame front boundary, as shown in Fig. 6c, of each image was extracted from the binary image. Fig. 6d–f shows the overlaying of the numbers of 5, 200 and 500 extracted flame front boundaries. It can be seen that 500 OH-PLIF images are sufficient to reflect the reaction region of the turbulent premixed flames. Therefore, ensemble averaging of instantaneous binary map of 500 OH-PLIF images was used to produce the smooth map of the Reynolds-averaged reaction progress variable, $\langle c \rangle$, from 0 to 1. $\langle c \rangle$ indicates the probability of the flame front location of the turbulent premixed flames. In this study, $\langle c \rangle$ = 0.1, 0.5, 0.9 are considered as unburned side, mean flame front location and burned side, respectively. The contour of $\langle c \rangle$ = 0.1, 0.5 0.9 and the mean flame cone of $\langle c \rangle$ = 0.1 are shown in Fig. 6g. Detailed calculation methods of S_T, Σ, and V_f will be described in the relevant sections.

4. Results and discussions

4.1. OH-PLIF images of turbulent premixed CH_4/H_2/air flames

Fig. 5a gives the direct image of the turbulent premixed flame. Even though the flame brush is clearly demonstrated, the detailed information such as flame front structure cannot be obtained. The typical OH-PLIF images of the turbulent premixed flames in this study at low turbulence intensity ($u'/S_L \approx 0.20$), intermediate turbulence intensity ($u'/S_L \approx 0.80$) and high turbulence intensity ($u'/S_L \approx 1.35$) are shown in Fig. 5b. Flames at different ZH_2 are shown in Fig. 5c and d. Although flame height varies with the flow conditions, the flame front tends to be much finer and more wrinkled with the increase of turbulence intensity and hydrogen fraction. In particular, those images show sharp ridges of high negative curvature surrounding large pockets of modest positive curvature. Here, curvature is defined as that positive curvature is convex with respect to reactants. The thin ridges may burn through to detach portions of the flame surface to form small islands under high turbulence condition ($u'/S_L \approx 1.35$) as shown in Fig 5b. Flame height tends to increase with the increase of turbulence intensity while decrease with the increase of hydrogen fraction. This is a general observation of the OH-PLIF images and more discussion will be made based on the quantitative flame front structure parameters in the later section. Fig. 5e shows the flame at $u'/S_L \approx 0$ without a perforated plate. Flame wrinkles caused by intrinsic flame instability are clearly seen at the tip of the flame. This means that intrinsic flame instability which influences the flame–turbulence interaction plays a significant role in the case of H_2 blending even though without turbulence.

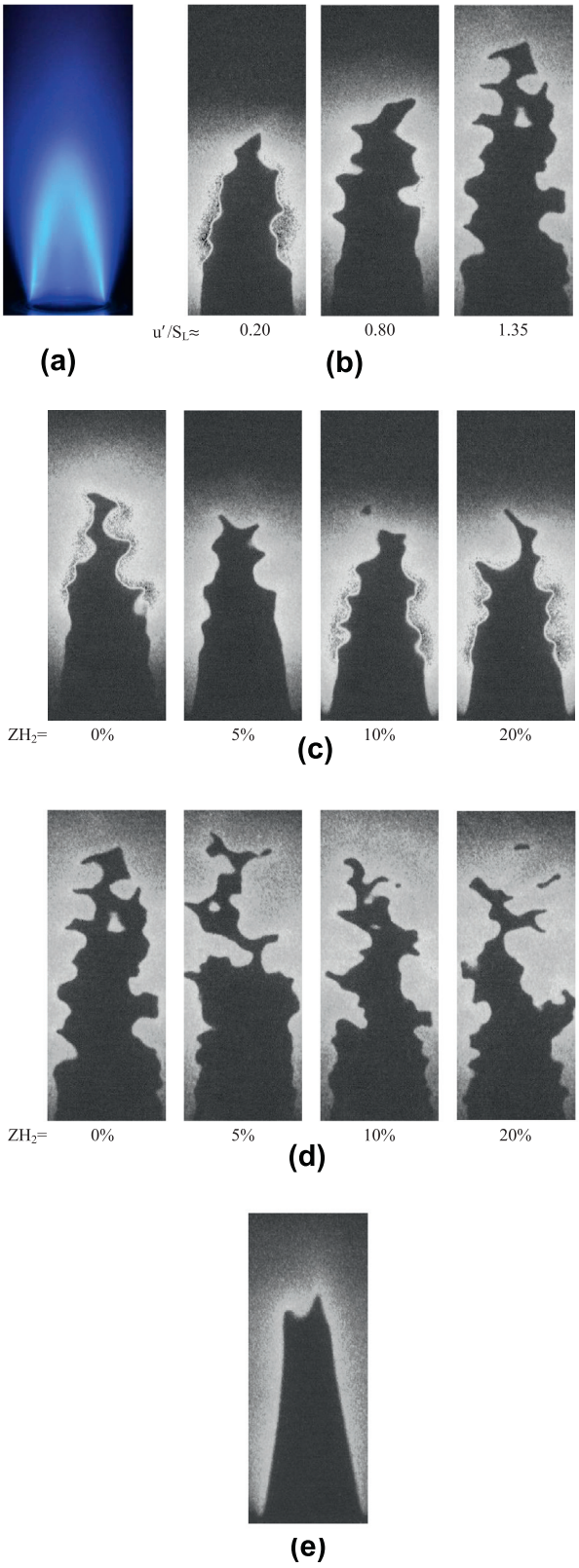

Fig. 5. OH-PLIF images of the turbulent premixed flames under various turbulence conditions and hydrogen fractions: (a) direct image by digital camera; (b) $u'/S_L \approx 0.25$; (c) $u'/S_L \approx 1.35$; (d) ZH_2 = 0%, $u'/S_L \approx 0$; (e) ZH_2 = 0%.

4.2. Effect of hydrogen addition on turbulent burning velocity

Fig. 6a gives the representative instantaneous flame front boundary of the single shot OH-PLIF image. Fig. 6d-f gives the

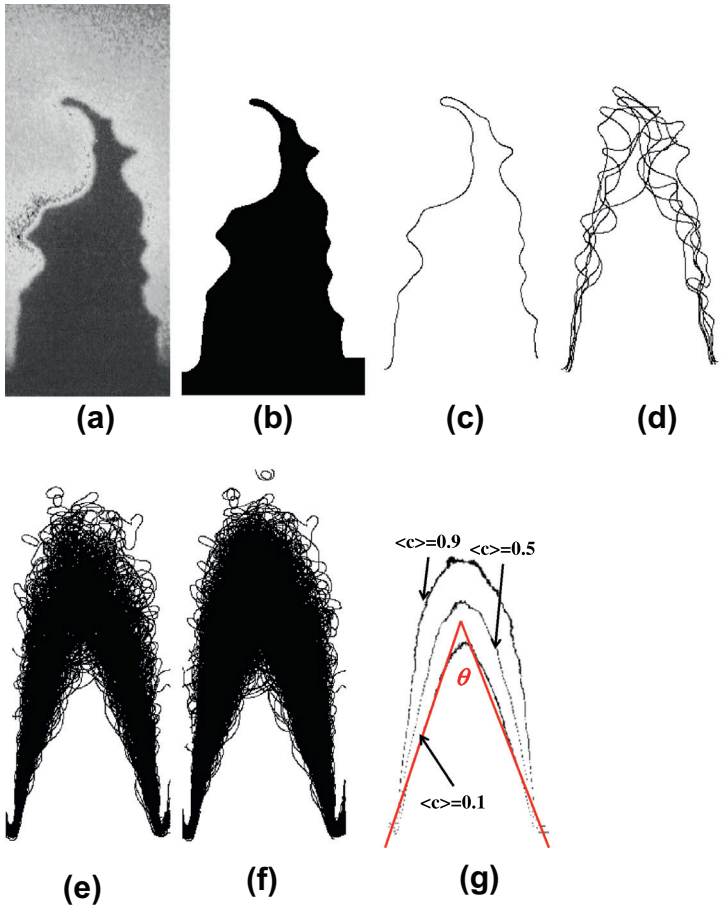

Fig. 6. Procedures of the image processing to track the instantaneous flame front and determine the mean flame cone at ⟨c⟩ = 0.1: (a) single shot OH-PLIF image; (b) binary map; (c) flame front boundary; (d)–(f) overlaying of a number of 5, 200 and 500 flame front boundaries and (g) contour of ⟨c⟩ = 0.1, 0.5 0.9.

superimposed instantaneous contours of convoluted thin reaction zones. It is seen that the positions of the reaction zone move rapidly in space, producing an apparently time averaged thick reaction zone which is frequently referred to as turbulent flame brush as shown in Fig. 6f. OH radical concentration increases quickly at the flame front. As discussed before, $\langle c \rangle = 0.1$ can be viewed as the averaged inner flame front of the turbulent premixed flames. The turbulent burning velocity, S_T, is obtained with conventional angle method [32] for the inner flame front, as

$$S_T = U \sin(\theta/2) \tag{2}$$

where θ is the cone angle (Fig. 6g), U is the mean velocity of the mixture at burner exit.

Fig. 7 gives the comparison of turbulent burning velocities of CH_4/air flames obtained in the present study with those of previous studies [31,33,34]. All data show a reasonable agreement within the experimental range. Fig. 8 [21] gives the variations of turbulent burning velocity, S_T, with the turbulence intensity, u', normalized by laminar burning velocity S_L. S_T/S_L significantly increases with

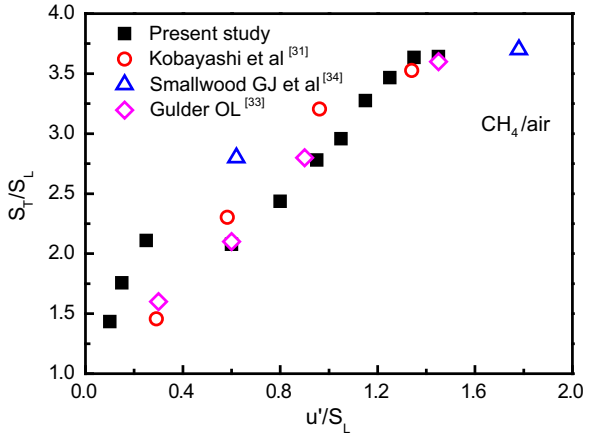

Fig. 7. Comparison of turbulent burning velocity with previous studies.

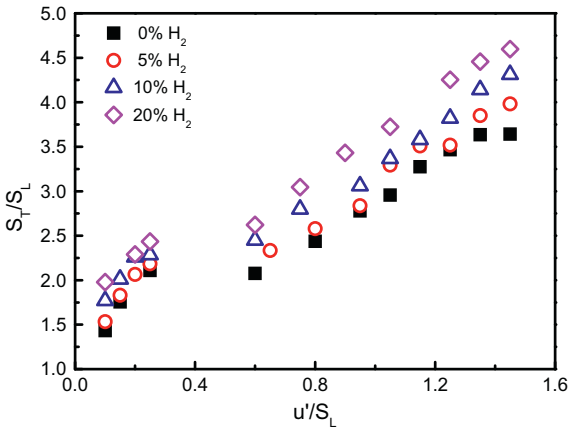

Fig. 8. Relationship between S_T/S_L and u'/S_L under various conditions [21].

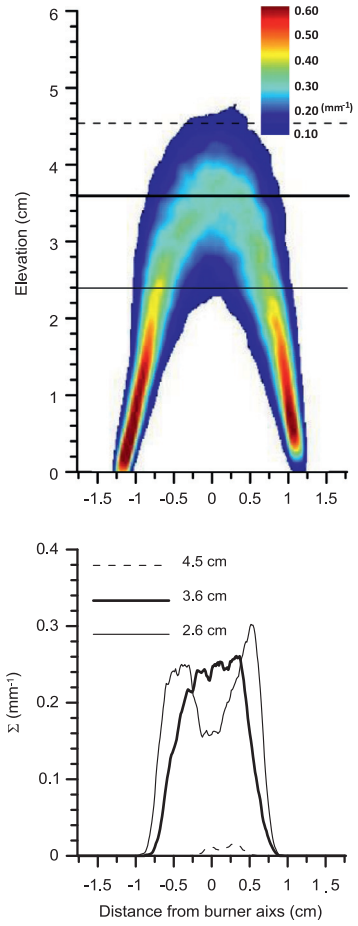

Fig. 9. Flame surface density at different elevation from the burner outlet.

the turbulence intensity and S_T/S_L is higher for the mixtures with higher hydrogen fraction under all conditions in the experimental range, even though all mixtures have the same laminar burning velocity. The turbulent premixed flames investigated here are located in the flamelet regime [29], as shown in Fig. 4. The increase of turbulent burning velocity in the flamelet regime is mainly due to not only the increase of flame front area caused by the turbulence wrinkling but also the stretched local laminar burning velocity considering the stretch effect. u'/S_L increase induces a large decrease of small turbulent scales. As a result, smaller flame surface elements dominate the turbulent flame structure, leading to finer wrinkles or larger flame front area and consequently increase the burning velocity. The production of small scale wrinkles can also be interpreted by characteristic flame instability scale, l_i, which is highly affected by Lewis number, Le_{eff}, and decreases with hydrogen ratio. l_i and Le_{eff} are listed in Table 1. The local burning velocity, S_{Lk} can be connected with S_L by the follwing equation:

$$S_L - S_{Lk} = L_M \alpha \tag{3}$$

α is the stretch rate and L_M represents the Markstein length calculated by $L_M = \delta_L Ma$, where δ_L is flame thickness and Ma is Markstein number. L_M is given in Table 1. L_M slightly decreases with the increase of hydrogen addition and this agrees well with the previous research [8]. Local burning velocity slightly decreases with the increase of stretch rate. This reveals that local turbulent flame front is not passively so much responding to the turbulent vortex motion. Thus, the increase in flame front area is the dominant factor in determining the S_T. Moreover, only 5% hydrogen addition can lead to an obvious difference to that of CH_4/air mixture. This suggests that hydrogen addition can significantly influence the flame characteristics and subsequently results in different turbulence–flame interaction, and this will be discussed in the later section based on the quantitative flame front structure parameters.

4.3. Effect of hydrogen addition on flame surface density

The mean reaction rate in turbulent premixed combustion related to flame surface density is expressed as [35]:

$$\dot{\omega} = \rho_u S_L I_0 \Sigma = \rho_u S_{Lk} \Sigma \tag{4}$$

where ρ_u is the density of unburned gas, S_L is the unstretched laminar burning velocity, while I_0 is the mean stretch factor, and Σ is the flame surface density. Laminar burning velocity considering the stretch effect, S_{Lk}, is an averaged value over all flame fronts. The flame surface density is defined as

$$\Sigma = \lim_{\Delta x \to 0} \frac{\bar{A}_f}{\Delta x^3} \cong \lim_{\Delta x \to 0} \frac{\bar{L}_f}{\Delta x^2} \tag{5}$$

where $\bar{A}_f$ and $\bar{L}_f$ are the time-averaged surface area and time-averaged surface length of flamelets within the control volume or the control area of size Δx, respectively. In the experimental study, information is available only in the plane of a laser sheet, so the following 2-D approximation is made usually.

Once flame front boundary is detected, the flame surface density, Σ, is calculated by the method of Filatyev et al. [36]. To determine Σ, it is assumed that the average flame surface area per unit volume equals the average flame perimeter per unit area in the laser sheet. At each location of interest, an interrogation box of size 11×11 pixel (resolution is about 0.136 mm) was chosen to cover the entire image pixels one by one. The length of the boundary was calculated in interrogation box by counting the number of pixels in the box. The final average flame length of 500 images divided by the area of the interrogation box is the flame surface density at the center of the box. The flame surface density field and profiles of flame surface density (Σ) are given in Figs. 10 and 11 at various hydrogen fractions and $u'/S_L \approx 0.20, 0.80, 1.35$, respectively.

The typical flame surface density field obtained from 2-D OH-PLIF images of turbulent premixed CH_4/air flames in this study is shown in Fig. 9 corresponding to the flame brush in Fig. 6f, which approximately indicates the brush thickness and shape of flame. The density field in Fig. 9 displays two peaks of Σ at the upstream locations (the thin solid line) corresponding to the two flame brushes that are stabilized on the right and left of Bunsen burner and it is axisymmetric about the burner axis. The peaks in two roots vanish further downstream and merge into one thick profile (the thick solid line). The profiles in different elevations in current study show a good agreement with the DNS simulation results of a slot flame reported by Bell et al. [18]. Fig. 10 indicates that Σ is increased while flame height is decreased with the increase of hydrogen fraction. And the flame surface density filed in Fig. 10 shows its maximum value in the center of the flame brush. It is confirmed in Fig. 11 which shows variations of the measured Σ as a function of mean progress variable $\langle c \rangle$. The Σ profiles are symmetric and have a maximum value at about $\langle c \rangle = 0.5$. Hydrogen addition slightly enhances the Σ and this tendency is more obvious under higher turbulence intensity ($u'/S_L \approx 0.80, 1.35$) as shown in Fig. 11a–c. This is due to the enhancement of the flame instability represented by effective Lewis number, Le_{eff}, and flame intrinsic instability scale, l_i. However, Σ tends to slightly decrease with the increase of turbulence intensity and seems to show an inverse tendency in Fig. 5b. As discussed before, large decrease of small turbulent scales is induced with increase of u'/S_L. Those scales result in smaller surface elements which dominate the turbulent flame structure, and consequently increase the flame wrinkles. To verify this, quantitative study of the flame wrinkle scale is required in the future. However,

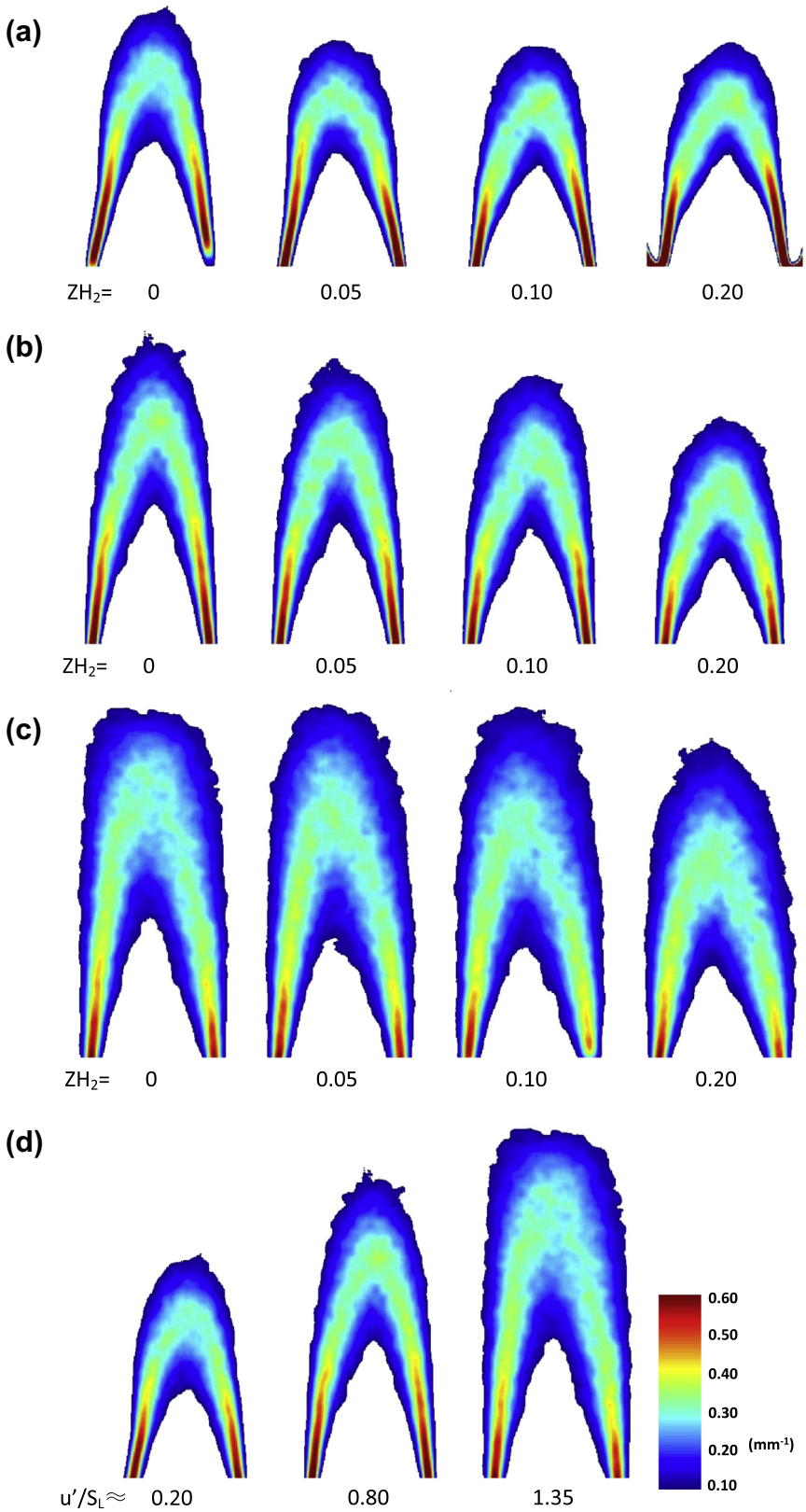

Fig. 10. Flame surface density field based on OH-PLIF images: (a) $u'/S_L \approx 0.20$; (b) $u'/S_L \approx 0.80$; (c) $u'/S_L \approx 1.35$ and (d) $ZH_2 = 0\%$.

Fig. 5b also shows that elevated turbulence intensity can enlarge the heat release region represented by mean flame volume, V_f, as shown in Fig. 12. That is, higher Σ is caused by smaller V_f and fineness of the small scale wrinkles and V_f is a dominant factor in this case.

4.4. Effect of hydrogen addition on mean flame volume

The averaged heat release rate in the turbulent flame region is proportional to the mean fuel consumption rate, $\langle W \rangle$, which is defined for lean mixture as follows [19]:

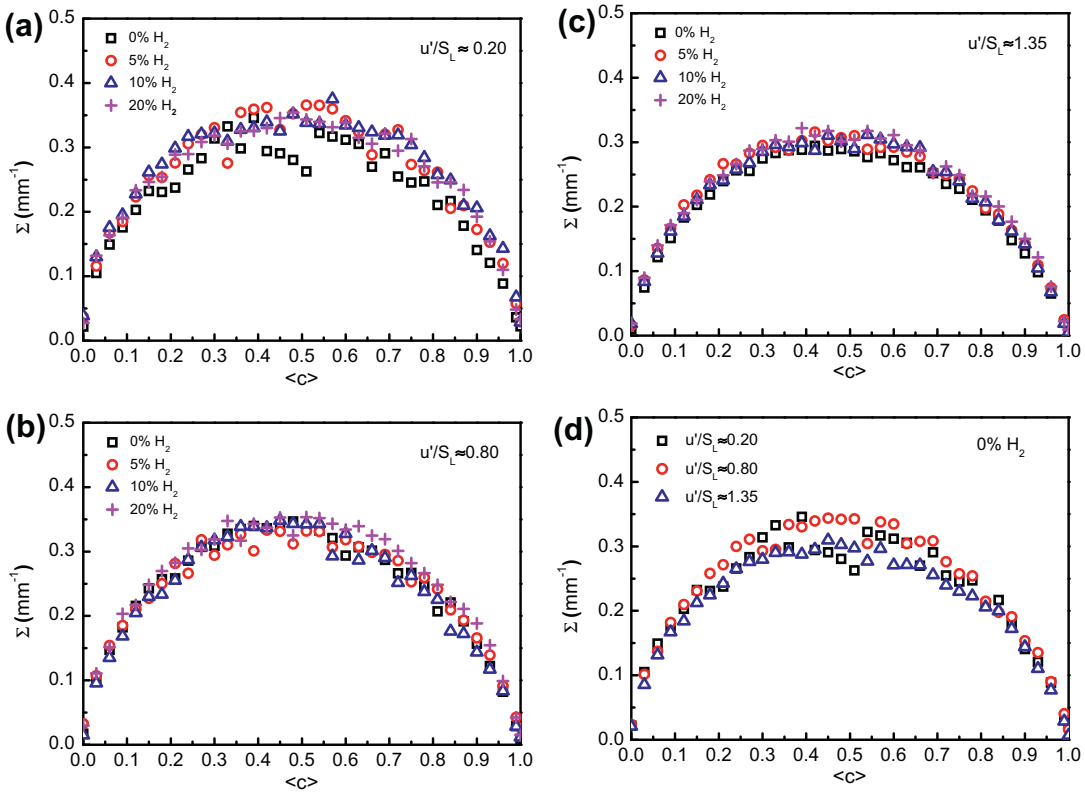

Fig. 11. Flame surface density versus ⟨c⟩ under different conditions.

$$\langle W\rangle = \rho_0 Y_f UA/V_f \tag{6}$$

where ρ_0 is the density of the mixture, Y_f is the mass fraction of the fuel, U is the mean velocity at the burner outlet, and A is the area of the burner outlet. The heat release profiles can be connected to combustion oscillation in the premixed-type combustors, such as gas-turbine. In this study, the mean volume of the turbulent flame region, V_f, as the heat-release region is measured by processing OH-PLIF images.

The mean volume of the turbulent flame region, V_f, is measured as follows. Firstly, the contour of $\langle c\rangle = 0.1$ from the burner outlet is divided into two parts at the flame-center axis, with these two parts being superimposed on each other. A polynomial curve with order of more than three is derived by the method of least squares for the superimposed $\langle c\rangle$ curves. The volume is then calculated by integrating the region after the polynomial curve is rotated numerically around the flame-center axis. The same procedure is employed for the contour of $\langle c\rangle = 0.9$. Secondly, the volume for $\langle c\rangle = 0.1$ is subtracted from that of $\langle c\rangle = 0.9$, and the volume of the turbulent flame region, V_f, is derived. The integral flame surface density in the region outside contours of 0.1 and 0.9 is much small enough compared to that in the inside region [35].

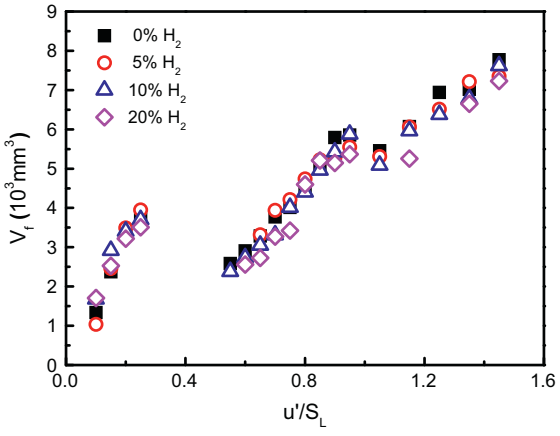

Fig. 12. Mean flame volume versus u'/S_L.

Fig. 12 shows the variations of the normalized turbulence intensity, u'/S_L, and mean flame volume, V_f, and the effect of hydrogen addition. V_f increases quickly with the increase of u'/S_L within the experimental range and this is mainly due to the increase in depth of the large scale flame wrinkles and the increase in flame height with u'/S_L. This is also the main reason for the decrease of flame surface density with the increase of u'/S_L. V_f remains almost constantly at various hydrogen fractions and this is due to the invariation of Markstein length, with the variation of hydrogen fraction. This indicates the passivity of the local flame front against flow turbulence at four hydrogen fractions is barely changed. This reveals that hydrogen addition is not the predominant parameter to influence the V_f of Bunsen-type turbulent premixed flame within the experimental range in this study.

5. Conclusions

Instantaneous flame front structure of turbulent premixed flames of the CH_4/H_2/air mixtures was studied quantitatively using a nozzle-type Bunsen burner with OH-PLIF technique. Quantitative parameters of flame front structure such as turbulent burning velocity, flame surface density, and mean flame volume were measured based on OH-PLIF images. And main results are summarized as follows:

(1) Flame front structures of turbulent premixed flames are the wrinkled flame front and the wrinkle intensity of flame front is promoted with the increase of turbulence intensity as well as hydrogen fraction.
(2) S_T/S_L increases significantly with the increase of turbulence intensity and increases slightly with the increase of hydrogen fraction. It is mainly due to the increased turbulent flame front area caused by the decrease in small scale of flame front structure and the slightly decreased local burning velocity.
(3) Flame surface density profile are symmetric and gives its maximum value at about $\langle c \rangle = 0.5$. Hydrogen addition slightly enhances the Σ and the tendency is more obvious under higher turbulence intensity due to the decrease of flame intrinsic instability. The decrease of Σ with the increase of turbulence intensity is due to the effect of enlarged flame volume.
(4) The mean flame volume of flame region apparently is increased with the increase of turbulence intensity within the experimental range due to the increase in depth of large scale flame wrinkles and the increase in flame height.

Acknowledgements

This study is supported by National Natural Science Foundation of China (Nos. 51006080, 51376004) and the Fundamental Research Funds for the Central Universities. Jinhua Wang acknowledges the Japan Society for the Promotion of Science for a JSPS Postdoctoral Fellowship grant.

References

[1] S.O.B. Shrestha, G.A. Karim, Hydrogen as an additive to methane for spark ignition engine applications, Int. J. Hydro. Energy 24 (1999) 577–586.
[2] S.R. Turns, Turbulent Premixed Flames, in: An Introduction to Combustion: concepts and applications, McGraw-Hill, Boston, 2000. pp. 158.
[3] S.R. Bell, M. Gupta, Extension of the lean operating limit for natural gas fueling of a spark ignited engine using hydrogen blending, Combust. Sci. Technol. 123 (1997) 23–48.
[4] E.J. Hu, Z.H. Huang, B. Liu, J.J. Zheng, X.L. Gu, Experimental study on combustion characteristics of a spark–ignition engine fueled with natural gas–hydrogen blends combining with EGR, Int. J. Hydro. Energy 34 (2009) 1035–1044.
[5] J.H. Wang, Z.H. Huang, C.L. Tang, J.J. Zheng, Effect of hydrogen addition on early flame growth of lean burn natural gas–air mixtures, Int. J. Hydro. Energy 35 (2010) 7246–7252.
[6] Z.H. Huang, J.H. Wang, B. Liu, K. Zeng, J.R. Yu, D.M. Jiang, Combustion characteristics of a direct-injection engine fueled with natural gas–hydrogen blends under various injection timings, Energy Fuels 20 (2006) 1498–1504.
[7] F.H. Ma, Y.F. Wang, S.F. Ding, L. Jiang, Twenty percent hydrogen-enriched natural gas transient performance research, Int. J. Hydro. Energy 34 (2009) 6523–6531.
[8] E.J. Hu, Z.H. Huang, J.J. He, C. Jin, J.J. Zheng, Experimental and numerical study on laminar burning characteristics of premixed methane–hydrogen–air flames, Int. J. Hydro. Energy 34 (2009) 4876–4888.
[9] M. Fairweather, M.P. Ormsby, C.G.W. Sheppard, R. Woolley, Turbulent burning rates of methane and methane–hydrogen mixtures, Combust. Flame 156 (2009) 780–790.
[10] M. Nakahara, T. Shirasuna, J. Hashimoto, Experimental study on local flame properties of hydrogen added hydrocarbon premixed turbulent flames, J Therm. Sci. Technol. 4 (2009) 190–201.
[11] R. Schefer, Hydrogen enrichment for improved lean flame stability, Int. J. Hydro. Energy 28 (2003) 1131–1141.
[12] P. Strakey, T. Sidwell, J. Ontko, Investigation of the effects of hydrogen addition on lean extinction in a swirl stabilized combustor, Proc. Combust. Inst. 31 (2007) 3173–3180.
[13] M. Mansour, Y.C. Chen, Stability characteristics and flame structure of low swirl burner, Exp. Therm. Fluid. Sci. 32 (2008) 1390–1395.
[14] A.W. Vreman, J.A. van Oijen, L.P.H. de Goey, R.J.M. Bastiaans, Direct numerical simulation of hydrogen addition in turbulent premixed Bunsen flames using flamelet-generated manifold reduction, Int. J. Hydro. Energy 34 (2009) 2778–2788.
[15] M.S. Day, X. Gao, J.B. Bell, Properties of lean turbulent methane–air flames with significant hydrogen addition, Proc. Combust. Inst. 33 (2011) 1601–1608.
[16] P. Dagaut, F.N. Egolfopoulos, Editorial Comment, Combust. Flame 159 (2012) 2531–2532.
[17] J.H. Wang, F. Matsuno, M. Okuyama, Y. Ogami, H. Kobayashi, Z.H. Huang, Flame front characteristics of turbulent premixed flames diluted with CO_2 and H_2O at high pressure and high temperature, Proc. Combust. Inst. 34 (2013) 1429–1436.
[18] J.B. Bell, M.S. Day, J.F. Grcar, M.J. Lijewski, J.F. Driscoll, S.A. Filatyev, Numerical simulation of a laboratory-scale turbulent slot flame, Proc. Combust. Inst. 31 (2007) 1299–1307.
[19] H. Kobayashi, H. Hagiwara, H. Kaneko, Y. Ogami, Effects of CO_2 dilution on turbulent premixed flames at high pressure and high temperature, Proc. Combust. Inst. 31 (2007) 1451–1458.
[20] Y.C. Chen, M.S. Mansour, Geometric interpretation of fractal parameters measured in turbulent Exp, Therm. Fluid. Sci. 27 (2003) 409–416.
[21] M. Zhang, J.H. Wang, Y.L. Xie, W. Jin, Z.L. Wei, Z.H. Huang, H. Kobayashi, Flame front structure and burning velocity of turbulent premixed CH_4/H_2/air flames, Int. J. Hydro. Energy 38 (2013) 11421–11428.
[22] U. Stopper, M. Aigner, H. Ax, W. Meier, R. Sadanandan, M. Stohr, A. Bonaldo, PIV, 2D-LIF and 1D-Raman measurements of flow field, composition and temperature in premixed gas turbine flames, Exp. Therm. Fluid. Sci. 34 (2010) 396–403.
[23] G. Coppola, A. Gomez, Experimental investigation on a turbulence generation system with high-blockage plates, Exp. Therm. Fluid. Sci. 33 (2009) 1037–1048.
[24] R.J. Kee, J.F. Grcar, M.D. Smooke, J.A. Miller, E. Meeks, A Program for Modeling Steady, Laminar, One-dimensional Premixed Flames, Sandia National Laboratories, Albuquerque, NM, 1985.
[25] R.J. Kee, F.M. Rupley, E. Meeks, J.A. Miller, A fortran chemical kinetics package for the analysis of gas-phase chemical and plasma kinetics, Sandia National Laboratories, Albuquerque, NM, 1993.
[26] G,P. Smith, D.M. Golden, M. Frenklach, N.W. Moriarty, B. Eiteneer, M. Goldenberg, C.T. Bowman, R.K. Hanson, S. Song, W.C. Gardiner, V.L. Jr., V.V. Lissianski, Z.W. Qin, GRI-Mech 3.0 Homepage, 1999, <http://www.me.berkeley.edu/gri_mech/>.
[27] J.K. Bechtold, M. Matalon, The dependence of the Markstein length on stoichiometry, Combust. Flame 127 (2001) 1906–1913.
[28] J. Yuan, Y.G. Ju, C.K. Law, On flame-front instability at elevated pressures, Proc. Combust. Inst. 31 (2007) 1267–1274.
[29] N. Peters, Turbulent Combustion, Cambridge University Press, Cambridge UK, 2000.
[30] H. Kobayashi, K. Seyama, H. Hagiwara, Y. Ogami, Burning velocity correlation of methane/air turbulent premixed flames at high pressure and high temperature, Proc. Combust. Inst. 30 (2005) 827–834.
[31] H. Kobayashi, T. Tamura, K. Maruta, T. Niioka, F.A. Williams, Burning velocity of turbulent premixed flames in a high-pressure environment, Twenty-Sixth Symp. (1996) 389–396.
[32] H. Kobayashi, Experimental study of high-pressure turbulent premixed flames, Exp. Therm. Fluid. Sci. 26 (2002) 375–387.
[33] Ö.L. Gülder, Turbulent premixed flame propagation models for different combustion regimes, in: Twenty-Third Symp. (Int.) on Combust., The Combustion Institute, Pittsburgh, 1990, pp. 743–750.
[34] G.J. Smallwood, Ö.L. Gülder, D.R. Snelling, B.M. Deschamps, I. Gökalp, Characterization of flame front surfaces in turbulent premixed methane/air combustion, Combust. Flame 101 (1995) 461–470.
[35] G.G. Lee, K.Y. Huh, H. Kobayashi, Measurement and analysis of flame surface density for turbulent premixed combustion on a nozzle-type burner, Combust. Flame 122 (2000) 43–57.
[36] S.A. Filatyev, J.F. Driscoll, C.D. Carter, J.M. Donbar, Measured properties of turbulent premixed flames for model assessment, including burning velocities, stretch rates, and surface densities, Combust. Flame 141 (2005) 1–21.